Received: July 18, 2022. Revised: September 7, 2022. 382

International Journal of
Intelligent Engineering & Systems

http://www.inass.org/

Breast Cancer Classification Using Customized ResNet Based Convolution Neural Networks

Nagaraja Rao Pamula Pullaiah[1]* **Dorai Venkatasekhar[2]**
Padarthi Venkatramana[3] **Balaraj Sudhakar[1]**

[1]*Department of Electronics & Communication Engineering, Annamalai University, India*
[2]*Department of Information Technology, Annamalai University, India*
[3]*Department of Electronics & Communication Engineering, Sree Vidyanikethan Engineering College, India*
* Corresponding author's Email: Nagaraj9s@gmail.com

Abstract: Deep learning is the most frequently used tool in the classification of tumors in medical applications. In recent decades, many research works have been done on the Breast Imaging Reporting & Data System (BI-RADS) atlas based classification of Breast cancer. As reported in the existing research works, training the larger datasets is a challenging task. Therefore, a customized ResNet based Convolution Neural Network (cRN-CNN) with batch normalization is proposed in this manuscript for addressing the above mentioned issue. The proposed cRN-CNN method has the advantage of faster training and computationally effective for the classification of BIRADS atlas based MRI breast cancer records, where the proposed model's performance is superior compared to the conventional CNN model. The extensive experiments performed on the Dynamic Contrast Enhanced-Magnetic Resonance Imaging (DCE-MRI) dataset confirmed that the proposed cRN-CNN method achieved better classification results than the existing methods. In the proposed model, the deformation technique based on elastic deformation is also applied to increase the training size of data that helps to improve the outcomes of prediction up-to 99.80%, because of the efficient strategy of batch normalization as customization and elastic deformation.

Keywords: Breast cancer, Batch normalization, Convolution neural network, Mammography, ResNet.

1. Introduction

Breast cancer is one of the most common types of cancer among females and an estimate of 268,600 new breast cancer patients have been diagnosed in the year 2019 [1]. On average 1 among 39 of the females who have breast cancer will die which is equals about 3% among diagnosed and 13% of diagnosed females who are suffering from an invasive type of breast cancer in their lifetime which equals nearly 1 out of 8 people. Breast cancer diagnosis concludes that the causes of death are from other sources and have an average risk than the lifetime risk of breast cancer. Screening mammography is one of the efficient and widely used methods for the detection of breast cancer [2]. There are two views included in the screening mammography of each breast namely a from top to bottom view called Cranio Caudal (CC) and an angle based side view called Medio Lateral Obligue (MLO). According to this visual examination, the radiologists will look for the symptoms of mammograms in the MRI images based on the BIRADS Atlas for mammogram descriptors [3, 4]. Some of the major descriptors namely calcifications, masses and architectural distortions are the common symptoms of breast cancer which are taken into account to standardize the terminology of the mammogram report and its corresponding evaluation and actions are to be taken. Radiologists prefer regular follow check-up or short-term check-ups based on the concern level of the cancer abnormality in the patient.

Severance of breast cancer can be analyzed through the detection of mammographic lesions by the automated computer aided detection (CAD) mechanism for the assistance of radiologists in taking

a decision and it only assists the radiologists, while the final call will be made by radiologists [5]. Numerous researchers have developed CAD systems for the detection of breast cancer by classifying it as benign masses or malignant masses [6]. But in general the Computerized diagnosis (CD) systems are not useful in the following check-ups of the patients like biopsy. As per the studies done there are less researches are being carried out based on BIRADS atlas for mammographic descriptors in classifying breast cancer effectively [7, 8]. In recent, deep learning based approaches have been utilized to show more efficient results nearer to the ground truth [9]. This research also proposes such a deep learning model with efficient data processing along with a customized ResNet based Convolution Neural Network (cRN-CNN) to obtain an accuracy of 99.8% which is better in comparison with the earlier studies [10]. The contribution of this research work is to provide a better localizing algorithm using cRN-CNN and to provide faster training using the transfer learning mechanism. Using the elastic deformation process of augmentation also provides a better training of MRI information for the proposed cRN-CNN network.

The organization of the paper is given as follows: Section 2 describes the Literature review on recent studies of breast cancer and its problems and Section 3 explains the functionalities of the proposed methodology and working of cRN-CNN Section 4 illustrates the experimental results and discussion. The conclusion of this research paper is given in Section 5.

2. Literature review

Akselrod-Ballin [11] proposed a modified region based convolution neural network for the identification and classification of mammographic masses using the BIRADS score. This method was applied to the data collected from a multi-centre clinic dataset and the results were evaluated for accuracy and efficiency of the proposed model. This method has a proficient impact on the growing nature of high volume and complex data in the health care models. The model has the disadvantage of taking larger time for training and it has to be applicable for multi-view datasets.

Cha [12] validated the deep learning models using the synthetic mammogram images to avoid the effects caused by overfitting of the model and to increase deep learning performance for breast cancer identification. Synthetic images were generated based on the silico procedure of breast analysis and the mass modeling techniques along with X-ray projection simulation of the breast as mammograms. In the phantoms of silico procedure, the mass contained was defined as four density descriptors of BIRADS which are based on variation in size, margin and shape for the masses. This method lacks the diversity of each category such as the shape and size of the breast and its characteristics also can affect lesser training results. Due to the computational complexity and limitation data categories for each combination which has been trained for evaluation.

Boumaraf [13] proposed an effective CAD model for the classification of mammographic masses based on the four assessment categories of BIRADS. The histogram equalization was used to enhance the regions and the region growing method was applied for the segmentation. The BIRADS descriptors such as shape, margin and density were extracted along with the patient's age based on the BIRADS mammography. A modified feature selection technique using a genetic algorithm has been applied to identify the most significant BIRADS descriptors for classification using a backpropagation based neural network and its accuracy value was taken as fitness for the genetic algorithm. The method has the drawback of using a conventional neural network rather than a deep architecture for the automated extraction of features from raw data.

Liu [14] investigated digital mammography based on the deep learning model for the prediction of malignant tumors using BIRADS microcalcifications. For this, a combined model using DL was created by including mammographic clinical variables. The model can improve the malignancy prediction by screening mammography and assisting the radiologists with better performance by facilitating the clinical decisions. The combined model focused more on the BIRADS microcalcifications detected by the radiologists and it needs more training for the accurate detection of tumors.

Yang [15] proposed a network called MommiNet which was a tri-view approach utilized for the detection of breast tumors. MommiNet detects tumors by performing the ipsilateral and bilateral analysis on the mammograms in parallel and enhancing the readability for the radiologists. This model has a network architecture with high resolution, symmetry, and geometry constraints based on learning information on the fully connected layers with respect to all the views for the accurate detection of mass. A learning approach based on multitasking is being incorporated into the BRADS descriptor-based malignancy classification network. MommiNet model has to be further improvised in performance

for malignancy detection in the different modality of images like MRI.

Sun, [16] developed three baseline CNNs with the same architectures, which were trained concurrently for predicting the sub-types of breast cancer. In this literature study, the classification and evaluation of the breast cancer sub-types were realized by fusing the prediction results of three baseline CNNs. Hence, the obtained experimental results confirmed that the developed model obtained high classification results on the DCE-MRI database by means of area under the curve, precision, accuracy, and specificity. Further, Zhang, [17] initially used a bounding box on the MRI images, which were collected from the DCE-MRI database. The RoI tumor regions were given as the input to the deep learning model named CNN with Convolutional Long Short Term Memory (CLSTM) for classifying the sub-types of breast cancer. Lastly, the transfer learning was employed for re-tuning the developed model, but it was computationally costly. To highlight the above stated problems, a novel cRN-CNN method is proposed in this manuscript.

3. Proposed methodology

Breast cancer is one of the most common types of tumor spread among the female breast and the world-wise cases have increased in total significantly since 1970. DCE-MRI dataset contains the intravenous injection of contrast agent which is paramagnetic and is characterized by wash-in and wash-out times specified. Vascularisation of tissues with physiological and morphological characteristics is highlighted by the contrast agent. Damage in tissues is identified by means of differentiating from the healthy tissues since tumors are solid, abnormal and irregular growth of blood vessels. DCE-MRI scan contains numerous 3D volumes of MRI taken from pre and post injection of the contrast agent resulting a 4D volume images with x,y, and z as spatial and t temporal dimension. Each pixel is related to the time-intensity curve which reflects the deviation of signal intensity caused by a release of the contrast agent over different 3D spatial dimensions and absorption. Even though malignancy lesion could be easily analysed visually for the difference between real and illustrative TIC, the huge variance between the subjects and larger data makes it hard for accurate and precise detection of malignancy, prone to errors and time taking tasks. To overcome these issues, CAD methods are being applied to detect lesions through computer vision by classification of lesions through automatic procedures. As many existing researches are being employed with hand-crafted image features some researchers are using DL based methods for classification. Among them, CNN has the advantage of utilizing hierarchical type of network structure which allows automatic learning of best features for malignancy detection but

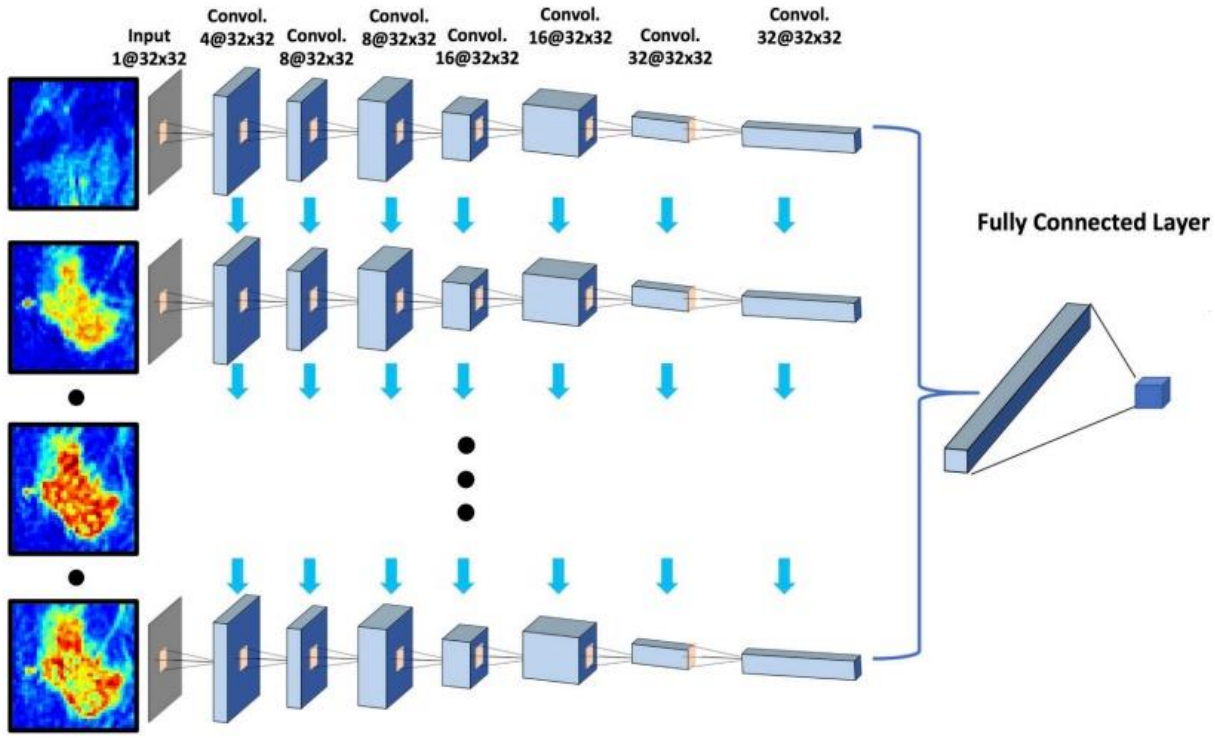

Figure. 1 Architecture of the proposed cRN-CNN method

requires more training data for better classification to converge. To overcome the approach of transfer learning is applied with a pre-trained model called ResNet 18 customized with batch normalization function in this research for a fine-tuned deep learning architecture for the malignancy detection. The proposed architecture of the cRN-CNN has been given in Fig. 1.

3.1 DCE-MRI dataset:

There are 55 anonymized DCE–MRI images of BC in the collection (11 images of DCIS and LCIS combination and 44 images of IDC). On a Philips Achieva 1.5 T MRI machine, the fat suppression based dynamic eThrive MRI sequence is formed. This technique considered images with at least one tumour mass, which is determined by a radiologist and confirmed by biopsy. In post-contrast pictures, an expert radiologist manually defined an ROI of the tumour mass for each slice. Before processing, the resampling of MRI volumes composes an isometric 1-mm pixel resolution. DCE-MRI is a time-based series of 3D pictures. The chosen technique processes the data of DCE-MRI in sequential form, to perform that the proposed algorithm cRN-CNN will become a natural choice to extract additional time-intensity information. However, the experiment discovered that the proposed network is difficult to train solely by using the label of the category. The variance of tumor detection precision is more significant, while the accuracy is low. As a result, the study approach adds a segmentation loss to the cRN-CNN output to aid training and focus the network's attention on the lesion region. Fig. 2 to 4 show examples of input photos and ground truth samples.

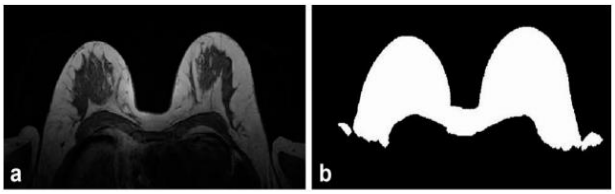

Figure. 2 Sample input image of MRI

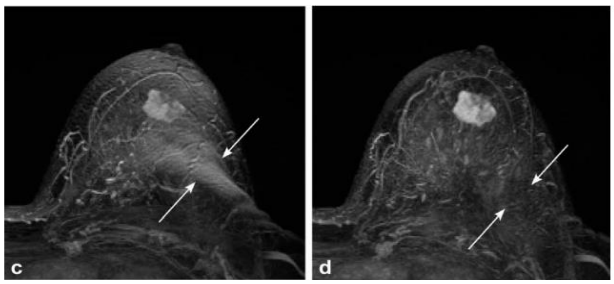

Figure. 3 Sample view of a tumor MRI slice

Figure. 4 Sample ground truth region of tumor

3.2 CNN and ResNet:

The traditional type of neural networks such as CNNs includes two major properties: sharing of weight and establishment of a connection local, which considerably improve their capacity to extract features while reducing the amount of training network parameters. In proposed CNN, the primary architecture contains input, output, fully-connected CNN layers and convolutional pooling layers with the layers taking the output from the previous layer as input feed to the current layer. In alternate layers, the convolution processor pooling process are employed in the structure. The major process of the CNN is Convolution layer function which maps the numerous features through its multiple neuron structure. While using a CNN to classify images, for instance, a CNN network layer reads the picture using the convolution function kernel and extracts image features using the information from neighboring regions in the image. The feature map of the picture is generated as follows after employing the activation function as shown in Eq. (1).

$$X_j^{l+1} = f\left(\sum_{i\epsilon M_j} \times k_{ij}^{l+1} + b_i^{l+1}\right) \quad (1)$$

Where, the j^{th} feature of the convolution layer is denoted as X_j^{l+1}, the features of input of the layer is denoted as X_i^l, and the rectified linear activation is represented as f, the set of input feature maps are said to be M_j, the offset variable is set as b and the operator $*$ as convolution process with k as kernel function for convolution. By reducing the dimension complexity of data and presenting with a higher level of features as in Eq. (2). For classifying images with the role of the pooling layer imitating the human vision mechanism convolution process is used.

$$X_j^{l+1} = X_j^l \otimes k_j^{l+1} + b_j^{l+1} \quad (2)$$

The three types of pooling algorithms are used majorly as maximum, median and average pooling

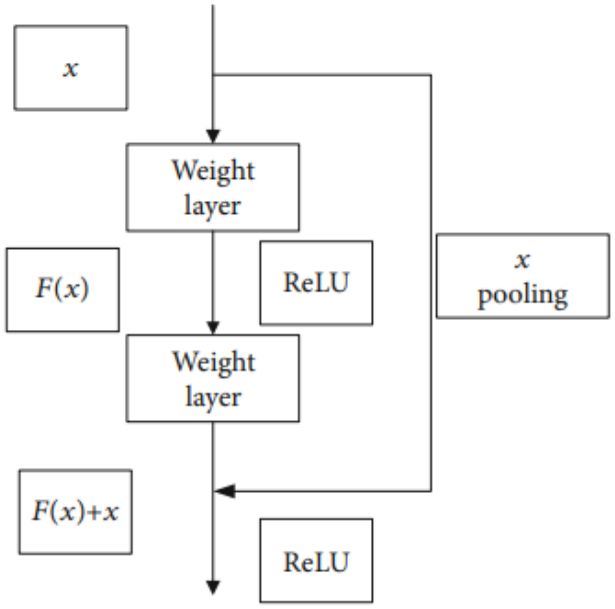

Figure. 5 cRN-CNN cell

and they are represented by the operator ⊗. The features trained to the layers are mapped to the label of class and the maximum likelihood process is used to calculate the value for each feature sample in the fully connected layer. From the calculation, it is observed that which label has the maximum likelihood, then the corresponding label is taken as classification output by the proposed model. The performance of the model is directly proportional to the depth of CNN layers along with the emergence of two major problems fades in gradient affecting the network convergence and the saturation of accuracy. Residual networks (ResNet) are gaining accuracy with more significance by increasing the number of layers and efficient tuning by resolving the problems of diminishing gradients and performance loss due to depth.

The element of ResNet is shown in Fig. 5 with the variable input X and targeted output H(x). The input x which is in the direct correspondence to the target output $[F(x) + x]$, obtains residue of $F(x) = H(x)$ as a shortcut link for the block for avoiding issues of accuracy saturation and depth rise. These links will interconnect 2 or more levels directly and immediately execute mapping of features. The model learns a reference (X) which is a residual function of each layer's input and this equation is less complex to optimize and increase the depth of network layers prominently as per Eq. (3).

$$F = W_2\sigma(W_1x) \tag{3}$$

Where the activation function ReLU is denoted with the term σ and the output can be acquired through an interconnected link and second unit of ReLU as mentioned in Eq. (4).

$$y = F(x, \{W_i\}) + x \tag{4}$$

When altering the dimensions of the input and the output (for example, altering the amount of channels), use the shortcut to perform a linear transformation function Ws to x as in Eq. (5):

$$y = F(x, \{W_i\}) + W_sx \tag{5}$$

ResNet models have 34 layers and 18 layers are developed for the analysis of ResNet building blocks as shown in Fig. 5 and as a result, the model ResNet-18 with 18 layers has been quicker in convergence than ResNet-34 with 34 layers.

3.3 Proposed cRN-CNN:

For the training of a neural network, a large number of data is required to improve the accuracy of a classification and the number of neurons in the hidden layer of the model. The dimension of neurons in the hidden layer grows with the growth in the dimension of input data in a fully connected network resulting rise in network parameters and training time of the model. A CNN model with local interconnection is proposed in this article due to its ability to share the characteristics of the parameter to reduce the number of network parameters required and to speed up the training time of the model. As a result, the design of the proposed model is improvised with the inclusion of ResNet-18 for the classification of breast cancer with BIRADS descriptor on the DCE-MRI dataset. The proposed model can extract more MRI data features from the input with an effective representation of its internal characteristics and thus it improves the accuracy. The cRN-CNN model was used to achieve precise detection and categorization of BIRADS descriptor-based classes in DCE-MRI dataset. Along with the compilation of pre-processing and training of cRN-CNN model, the optimizer algorithm and its loss function computation are employed as critical components of a network that allows CNN to handle the data efficiently. The optimizer settings are determined by the value of learning rate of the neural network. In the proposed method, Stochastic Gradient Descent (SGD) optimization is utilized with the key metric of loss function for assessing the model quality as cross entropy calculation. Learning rate value is determined as 0.1 in the initial stage and a step change is required in the follow-up for the better convergence of objective function. Within a 3-

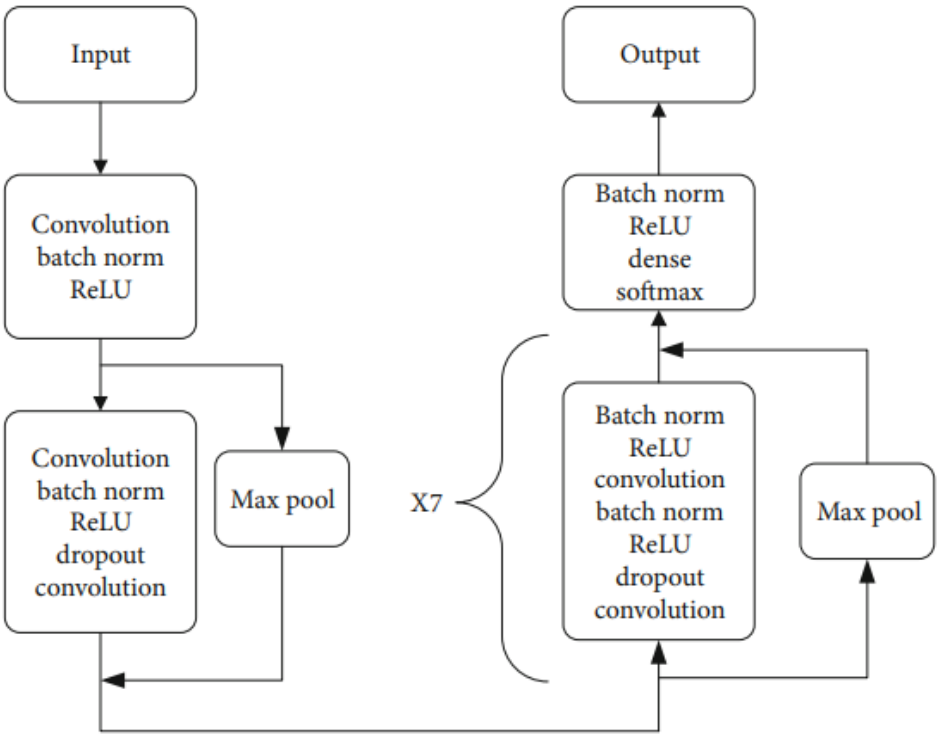

Figure. 6 Customized ResNet-CNN model

second frame, the MRI image data samples were segmented to produce 1080 sample points. When going through each convolutional layer, the quantity of convolutional starts at 12 and gradually grows. There are two output values since the modified ResNet-18 algorithm is presented for identifying the five primary BIRADS categories in MRI data. Each layer's dimensions and values are shown in Fig. 6. To extract the properties of the data input, a one-dimensional convolutional function kernel determined with a length of 32 is applied. For two-dimensional picture classification, the original ResNet-18 model tends to employ a tiny convolution function based kernel layer with a size of 33. The picture quality of the direct input values of the network is, on average, somewhat poor. The 33% area is likely to include considerable alterations even while the receptive region is at the value its smallest. The MRI data and the image data are fundamentally different. Such as in MRI, having just three dimension points at any one position, makes it impossible to generate a meaningful convolution change for low-resolution, pixel points. Furthermore, these signals are extremely vulnerable to interference of noise, which can have a major detrimental influence on feature learning and, in extreme circumstances, result in unsuccessful learning. As a result, for effective relief of this problem, the usage of a larger convolution kernel is discussed here.

The developed ResNet-18 model is divided into four parts: a convolution layer, a conventional ResNet-18 layer, an upgraded ResNet18 model layer, as well as a fully connected layer as shown in Fig. 6. For the processing of further levels deeper, the input image features are extracted from the initial block of the convolution layer. And the second layer has the ResNet-18 model with customization of batch normalization to recognize the finest informative features in MRI classification. Convolution with modified ReLU is done twice for the input in this section. The output of certain neurons from convolution layers is made zero by ReLU which will reduce the parameter dependency and resulting the network being sparse along with a reduction of the overfitting issue. The data are fed to a layer of maximum pooling before the layer of convolution to reduce the amount of work and number of parameters by splitting into feature regions of data samples and utilizing the one with maximum value as the representative of the region. In the end, two types of outputs with the same dimensions are being combined after processing significantly to finish the formation of the block module. In each phase, the optimization effect is carried over from previous to another and keeps the convergence of the model.

At section three, a customized ResNet-18 with batch normalization is employed to get higher performance, speed up the training of the network, boosting the convergence speed and algorithm

stability retention. And then the data is transmitted to the fully connected CNN layer then the entire model will pass through the data structure seven times. Finally, the features obtained from the output layer are converted to a dimension vector for which the softmax regression function is applied which has the nature of multiobjective classification. Conversion of n-dimension vector to another vector of n-dimension and transforming it as a representation of the output feature with the fully connected layer is the goal of using an exponential function. All the results are summated and normalized to render the findings of multiclassification from the structure of probability. Eq. (6) defines the softmax function as follows.

y=CNNfeatures

$$p_i = softmax(\lg_i) = \frac{e^{\lg_i}}{\sum_{i=0}^{n-1} e^{\lg_i}}$$
$$ls_i = \sum_{i=0}^{n-1} y_i \times \ln p_i \quad (6)$$

The corresponding label of breast tumor type is represented as CNN features and its label is y, with the presence of breast tumor as per BIRADS descriptor it is mentioned as class label 1 and with the absence of breast tumor it is specified as class label 0, and n is the number of breast tumor types to be classified while the probability of classification to each type be p_i. The corresponding state l_{si} and vector output for the i^{th} value is defined as l_{gi}. The translated output vectors from features are converted to one-dimension vector and are being generated using the function of softmax activation based upon the training images convolution, regularization, activation, and pooling. In end the breast tumor classification is depicted as a chart of probability. L2 regularization is being applied in the proposed model to all convolution and fully-connected layers increasing network convergence speed and avoiding overfitting problems. The equation for the weight regularization loss function is given in Eq. (7).

$$Loss = (\theta - W^T x)^2 + \alpha||W||^2 \quad (7)$$

Where α is the regular term coefficient, W is the weight of the network, θ is the image category prediction value, x is a feature of the image sample data, and T is the amount of weighted elements. The convolutional layer was given a dropout (0.5) to reduce the dimensionality of parameters and the training time utilized. The updated ResNet-18 model was utilized in the studies to categorize heartbeats in MRI images from DCE-MRI BIRADS data collection. Although the density of the spatial-temporal dimension makes it hard for the human eye to differentiate particular places in MRI pictures, with the aid of the developed model identification of the tag in each marker image may be easier. The suggested model can classify complicated mixed wave pictures in a quicker computing time than previous classification models. The model training has been completed as shown in Fig. 7 and 8.

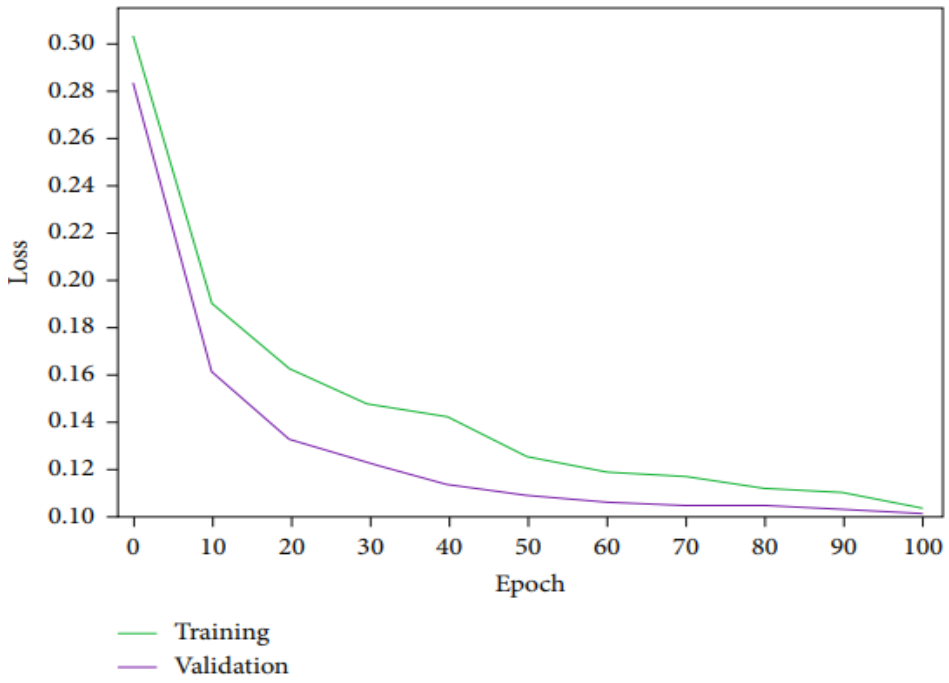

Figure. 7 Loss vs Epochs

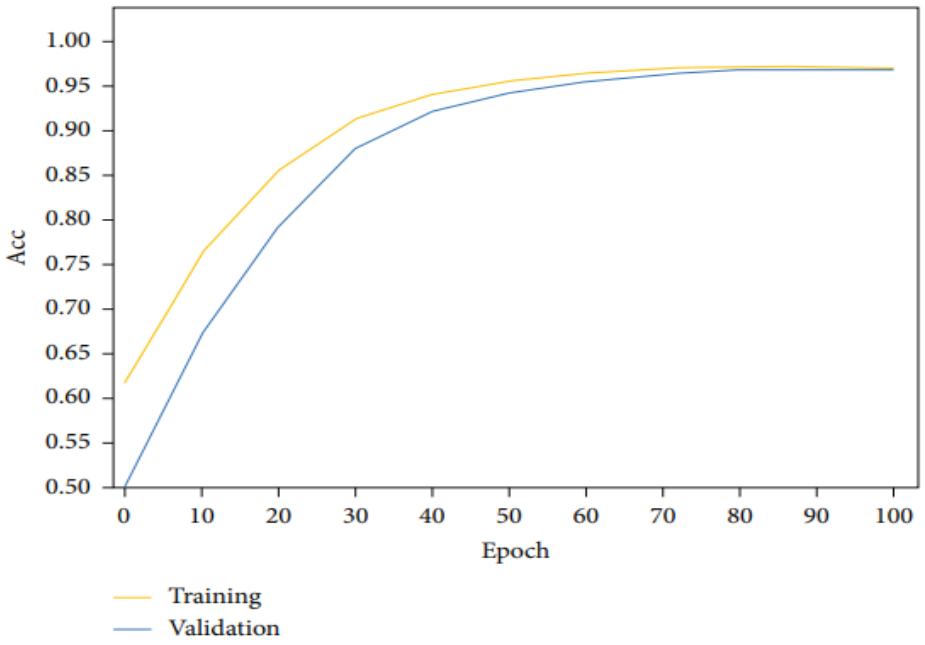

Figure. 8 Accuracy vs Epochs

4. Experimental results and discussion

The research discusses the specifics of the experiments and assesses the outcomes in this section. The parameters of the learning rate, number of steps, momentum and batch size is determined as 0.001, 0.0005,50 and 0.9 respectively as per the gradient descent tuning. During the process of training, data augmentation is being used which includes randomized flip and randomized crop (242424). Data is clipped at the center 242424 portions during testing. To assess the network's performance, we employ cross-validation (k = 3), using training and test sets collected as types of benign data samples and malignant data samples, respectively. The Metrics like Accuracy, Precision, and Recall are being evaluated and the formula for the metrics is given as shown in Eqs. (8) to (10).

$$Accuracy = \frac{TP+TN}{TP+TN+FP+FN} \times 100 \quad (8)$$

$$Precision = \frac{TP}{TP+FN} \times 100 \quad (9)$$

$$Recall = \frac{TN}{TN+FP} \times 100 \quad (10)$$

Here, the True Positive samples are represented as TP, False Positive samples are represented as FP, True Negative samples are represented as TN and False Negative samples are denoted as FN. cRN-CNN model's initial position during the classification of MRI is initialized with the parameters as above mentioned in the research. After to finalize the values of parameters is utilized by the proposed network with computed loss function for classification.

Table 1. Experimental analysis of various models

Network	Accuracy (%)	Precision (%)	Recall (%)
ResNet18	82.5	80	86.6
CNN	86.7	86.7	85.6
Customized ResNet18	93.6	91.7	97.8
cRN-CNN	99.8	99	98.7

Table 1 shows the categorization findings. The baseline is handled as ResNet. The precision, recall and classification accuracy of DCE-MRI are enhanced using the CNN model with the function of ResNet 18 model to encode the data. The proposed cRN-CNN achieves the greatest results with noticeable gains. Subtracting the values of the second column from the first helps its absolute value which will give the weight of each feature for each job in a ResNet-50 model with a 20482 matrix of its own fully connected layer. This demonstrates a strong link between the core job and the auxiliary duties. The weight values of cRN-CNN are less than those of ResNet, implying that generalizability is improved. The major difference is that in the primary task, the top ten weights aren't as significant as they are in the supplementary tasks. For the main objective task weight significance is improved irrespective of subtasks by involving major diagnostic features of data like pixel value and curve of time-intensity.

In addition, Table 2 states the comparative results of the proposed model and the existing models: CNNs with ensemble learning [16] and CNN-CLSTM [17]

Table 2. Comparative results of the proposed model and the existing models

Network	Dataset	Accuracy (%)	Precision (%)	Recall (%)
CNNs with ensemble learning [16]	DCE-MRI	85.20	96.10	-
CNN-CLSTM [17]		92	-	90
cRN-CNN		99.8	99	98.7

on the DCE-MRI dataset. The CNNs with ensemble learning model has achieved classification accuracy of 85.20% and precision of 96.10% on the DCE-MRI dataset. In addition, the CNN-CLSTM achieved 92% of classification accuracy and 90% of recall on the DCE-MRI dataset. Related to these existing models, the proposed cRN-CNN model has achieved higher classification results. As denoted earlier, cRN-CNN model is computationally effective related to the comparative models, which is the major problem highlighted in the literature section.

5. Conclusion

This research presents a strategy for classifying benign and malignant tiny lesions of tumors in DCE-MRI database of breast cancer with two elements to the process. In this research, an effective framework named cRN-CNN for the classification of DCE-MRI dataset based on BIRADS descriptor is proposed. The proposed cRN-CNN improves the value of accuracy from 73 to 99.8% when tested on our dataset. This research proposed latent characteristics learning approach in response to the hard-training challenge. The proposed cRN-CNN approach effectively utilizes information from reports of diagnostics and outcomes of medical analysis along with accelerating network convergence. In the future, fine-tuning of the parameters of the proposed cRN-CNN model can be carried out for the effective performance and reduced complexity of analysis.

Conflicts of Interest

The authors declare no conflict of interest.

Author Contributions

The paper conceptualization, methodology, software, validation, have been done by 1st author formal analysis, investigation, resources, data curation have been done by 2nd author writing—original draft preparation, writing—review and editing, visualization, have been done by 3rd author. The supervision and project administration, have been done by 4th author.

References

[1] M. E. Adoui, S. A. Mahmoudi, Larhmam, and M. Benjelloun, “MRI breast tumor segmentation using different encoder and decoder CNN architectures”, *Computers*, Vol. 8, No. 3, p. 52, 2019.

[2] C. Haarburger, M. Baumgartner, D. Truhn, M. Broeckmann, H. Schneider, S. Schrading, C. Kuhl, and D. Merhof, “October. Multi scale curriculum CNN for context-aware breast MRI malignancy classification”, In: *Proc. of International Conference on Medical Image Computing and Computer-Assisted Intervention*, pp. 495-503, 2019.

[3] X. Zhou, F. Gao, S. Duan, L. Zhang, Y. Liu, J. Zhou, G. Bai, and W. Tao, “Radiomic features of Pk-DCE MRI parameters based on the extensive Tofts model in application of breast cancer”, *Physical and Engineering Sciences in Medicine*, Vol. 43, No. 2, pp. 517-524, 2020.

[4] H. M. Whitney, H. Li, Y. Ji, P. Liu, and M. L. Giger, “Comparison of breast MRI tumor classification using human-engineered radiomics, transfer learning from deep convolutional neural networks, and fusion methods”, In: *Proc. of the IEEE*, Vol. 108, No. 1, pp. 163-177, 2019.

[5] D. K. Patra, T. Si, S. Mondal, and P. Mukherjee, “Breast DCE-MRI segmentation for lesion detection by multi-level thresholding using student psychological based optimization”, *Biomedical Signal Processing and Control*, Vol. 69, p. 102925, 2021.

[6] A. Hizukuri, R. Nakayama, M. Nara, M. Suzuki, and K. Namba, “Computer-aided diagnosis scheme for distinguishing between benign and malignant masses on breast DCE-MRI images using deep convolutional neural network with Bayesian optimization”, *Journal of Digital Imaging*, Vol. 34, No. 1, pp. 116-123, 2021.

[7] M. C. Comes, A. Fanizzi, S. Bove, V. Didonna, S. Diotaiuti, D. L. Forgia, A. Latorre, E. Martinelli, A. Mencattini, A. Nardone, and A. V. Paradiso, “Early prediction of neoadjuvant chemotherapy response by exploiting a transfer learning approach on breast DCE-MRIs”, *Scientific Reports*, Vol. 11, No. 1, pp. 1-12, 2021.

[8] R. Sumathi and V. Vasudevan, “MRI Breast Tumor Extraction Using Possibilistic C Means

and Classification Using Convolutional Neural Network", In: *Proc. of Micro-Electronics and Telecommunication Engineering*, pp. 795-803, 2022.

[9] A. H. Yurttakal, H. Erbay, T. İkizceli, and S. Karaçavuş, "Detection of breast cancer via deep convolution neural networks using MRI images", *Multimedia Tools and Applications*, Vol. 79, No. 21, pp. 15555-15573, 2020.

[10] G. Holste, S. C. Partridge, H. Rahbar, D. Biswas, C. I. Lee, and A. M. Alessio, "End-to-End Learning of Fused Image and Non-Image Features for Improved Breast Cancer Classification from MRI", In: *Proc. of the IEEE/CVF International Conference on Computer Vision*, pp. 3294-3303, 2021.

[11] A. A. Ballin, L. Karlinsky, S. Alpert, S. Hashoul, R. B. Ari, and E. Barkan, "A CNN based method for automatic mass detection and classification in mammograms", *Computer Methods in Biomechanics and Biomedical Engineering: Imaging & Visualization*, Vol. 7, No. 3, pp. 242-249, 2019.

[12] K. H. Cha, N. A. Petrick, A. X. Pezeshk, and C. G, "Evaluation of data augmentation via synthetic images for improved breast mass detection on mammograms using deep learning", *Journal of Medical Imaging*, Vol. 7, No. 1, p. 012703, 2019.

[13] S. Boumaraf, X. Liu, C. Ferkous, and X. Ma, "A new computer-aided diagnosis system with modified genetic feature selection for bi-RADS classification of breast masses in mammograms", *BioMed Research International*, Vol. 2020, 2020.

[14] H. Liu, Y. Chen, Y. Zhang, L. Wang, R. Luo, H. Wu, C. Wu, H. Zhang, W. Tan, H. Yin, and D. Wang, "A deep learning model integrating mammography and clinical factors facilitates the malignancy prediction of BI-RADS 4 microcalcifications in breast cancer screening", *European Radiology*, Vol. 31, No. 8, pp. 5902-5912, 2021.

[15] Z. Yang, Z. Cao, Y. Zhang, Y. Tang, X. Lin, R. Ouyang, M. Wu, M. Han, J. Xiao, L. Huang, and S. Wu, "MommiNet-v2: Mammographic multi-view mass identification networks", *Medical Image Analysis*, Vol. 73, p. 102204, 2021.

[16] R. Sun, Z. Meng, X. Hou, Y. Chen, Y. Yang, G. Huang, and S. Nie, "Prediction of breast cancer molecular subtypes using DCE-MRI based on CNNs combined with ensemble learning", *Physics in Medicine & Biology*, Vol. 66, No. 17, p. 175009, 2021.

[17] Y. Zhang, J. H. Chen, Y. Lin, S. Chan, J. Zhou, D. Chow, P. Chang, T. Kwong, D. C. Yeh, X. Wang, and R. Parajuli, "Prediction of breast cancer molecular subtypes on DCE-MRI using convolutional neural network with transfer learning between two centers", *European Radiology*, Vol. 31, No. 4, pp. 2559-2567, 2021.